MOLECULAR AND CELLULAR BIOLOGY, May 2008, p. 3410–3423 Vol. 28, No. 10
0270-7306/08/$08.00+0 doi:10.1128/MCB.01027-07

Regulation of the *Drosophila* Hypoxia-Inducible Factor α Sima by CRM1-Dependent Nuclear Export▽

Nuria M. Romero,[1] Maximiliano Irisarri,[1] Peggy Roth,[2] Ana Cauerhff,[1] Christos Samakovlis,[2] and Pablo Wappner[1]*

Instituto Leloir and FBMC, FCEyN, Universidad de Buenos Aires, CONICET, Patricias Argentinas 435, Buenos Aires 1405, Argentina,[1] and Department of Developmental Biology, Wenner-Gren Institute, Stockholm University, S-106 96 Stockholm, Sweden[2]

Received 11 June 2007/Returned for modification 28 August 2007/Accepted 25 February 2008

Hypoxia-inducible factor α (HIF-α) proteins are regulated by oxygen levels through several different mechanisms that include protein stability, transcriptional coactivator recruitment, and subcellular localization. It was previously reported that these transcription factors are mainly nuclear in hypoxia and cytoplasmic in normoxia, but so far the molecular basis of this regulation is unclear. We show here that the *Drosophila melanogaster* HIF-α protein Sima shuttles continuously between the nucleus and the cytoplasm. We identified the relevant nuclear localization signal and two functional *n*uclear *e*xport *s*ignals (NESs). These NESs are in the Sima basic helix-loop-helix (bHLH) domain and promote CRM1-dependent nuclear export. Site-directed mutagenesis of either NES provoked Sima nuclear retention and increased transcriptional activity, suggesting that nuclear export contributes to Sima regulation. The identified NESs are conserved and probably functional in the bHLH domains of several bHLH-PAS proteins. We propose that rapid nuclear export of Sima regulates the duration of cellular responses to hypoxia.

In eukaryotic organisms, transcription factors are typically regulated at the level of transcription or controlled through a wide variety of posttranslational mechanisms that frequently operate simultaneously to cope with dynamic cell needs. Regulation of transcription factor expression is a robust mechanism, usually associated with highly stereotyped processes, such as the development of multicellular organisms. Regulation through posttranslational modifications, such as phosphorylation, proteolytic processing, and control of subcellular localization, is less robust but allows for rapid responses that enable adaptation to external insults or modifications in the extracellular milieu. Therefore, the combination of transcriptional and posttranslational mechanisms that account for transcription factor regulation ensures an ample repertoire of responses that allows adaptation to diverse situations.

Transcription factors of the basic helix-loop-helix–PAS (bHLH-PAS) family control a wide array of biological functions throughout the animal kingdom, including different developmental processes, circadian rhythmicity, xenobiotic responses, and adaptation to hypoxia. bHLH-PAS proteins are α/β heterodimers in which α-subunits provide functional specificity and β-subunits are promiscuous partners, though absolutely necessary for transcriptional activity. Members of the bHLH-PAS family display an overall conserved modular structure characterized by several domains distributed in a highly stereotyped pattern along the protein (10, 26) (see Fig. 1A, below). The bHLH domain, typically localized to the N terminus, has a basic region (b) that consists of a stretch of 12 mainly basic residues that bind a G/CTAC-GTG consensus in the DNA, the asymmetric E-box (53, 56); the HLH component of the bHLH domain that is involved in α/β heterodimerization is a hydrophobic region of approximately 50 residues encompassing two amphipathic α-helices separated by a loop of variable length (37), and the PAS domain is another protein-protein interaction domain that contributes to defining target gene specificity (42). Finally, the glutamine-rich transcription activation domain is typically localized at the C terminus and interacts with the basic transcriptional machinery, thereby enabling transcription (37).

Those bHLH-PAS proteins that mediate developmental processes are mainly regulated at a transcriptional level. They display spatially and temporally restricted expression patterns that generally anticipate their developmental function. For example, the *Drosophila melanogaster* bHLH-PAS protein Trachealess, a master regulator of tracheal and salivary duct development, is expressed in embryonic tracheal and salivary duct precursors (20, 54); Dysfusion, another *Drosophila* bHLH-PAS transcription factor, is involved in tracheal fusion and is expressed exclusively in a specific subset of tracheal cells known as fusion cells (21). The same principle applies to bHLH-PAS proteins that control other developmental processes, such as the *Drosophila* and mammalian Single-minded proteins, which are involved in differentiation and development of the nervous system.

In contrast to bHLH-PAS proteins that mediate developmental processes, transcription factors of this family that regulate homeostatic responses to physiologic or environmental stimuli are controlled through a complex array of posttranslational mechanisms that fine-tune their transcriptional activity in response to these external cues (40, 41).

Hypoxia-inducible factors (HIFs) are a family of mammalian bHLH-PAS proteins that mediate adaptation to oxygen deprivation. Whereas the expression of their β-subunit, a common

* Corresponding author. Mailing address: Patricias Argentinas 435, Buenos Aires 1405, Argentina. Phone: (54-11) 52387500. Fax: (54-11) 5238-7501. E-mail: pwappner@leloir.org.ar.

▽ Published ahead of print on 10 March 2008.

partner of several other bHLH-PAS proteins, is unaffected by oxygen levels (50), the α-subunit is regulated by oxygen through several concurrent mechanisms that include control of protein degradation (7, 14, 34, 55), transcriptional coactivator recruitment (46), and regulation of subcellular localization (25, 49). The mechanisms underlying oxygen-dependent control of HIF-α protein stability and transcriptional coactivator recruitment have been well characterized. In contrast, the molecular basis of the regulation of HIF-α oxygen-dependent subcellular localization is unclear. Studies in mammalian cell lines have shown that HIF-α is mainly cytoplasmic in normoxia and nuclear in hypoxia; it has been proposed that this phenomenon involves hypoxia-dependent nuclear import (9, 25), which in turn depends on a conserved bipartite nuclear localization signal (NLS) mapping next to the C terminus of HIF-α-subunits (32).

Our group and other laboratories have defined a hypoxia-inducible transcriptional response in *Drosophila* that is homologous to mammalian HIF (7, 8, 12, 13, 16, 31). The *Drosophila* genes involved in the response have been defined, and they are *Drosophila* Tango (Tgo) (47) and Similar (Sima) (39) bHLH-PAS proteins, HIF-β and HIF-α homologues, respectively (7, 16, 31). Whereas Tgo is not regulated by oxygen, Sima protein is stabilized in hypoxia, with degradation in normoxia being dependent on a central domain encompassing amino acids 692 to 863 that are functionally homologous to the mammalian HIFα oxygen-dependent degradation domain (ODDD) (8, 31). Recently, we showed that continuous ectopic expression overrode Sima degradation, which remained mostly cytoplasmic in normoxia and accumulated in the nucleus in hypoxia (12). Regulation of subcellular localization is not an all-or-none response but, rather, depends on oxygen levels in a dose-dependent manner and is also modulated by developmental parameters during embryogenesis (12).

In this study we have further investigated the mechanism controlling HIF-α/Sima subcellular localization. We show that Sima shuttles continuously between the nucleus and cytoplasm. Nuclear import is mediated by a noncanonical bipartite NLS that maps next to the Sima C terminus. Nuclear export depends on two functional nuclear export signals (NESs) localized in the bHLH domain that are critically required for Sima steady-state subcellular localization and for nuclear export upon reoxygenation. These functional NESs are conserved in the bHLH domain of mammalian HIF-α subunits, as well as in several other bHLH-PAS proteins throughout evolution.

MATERIALS AND METHODS

DNA constructs. To generate the enhanced green fluorescent protein (EGFP)-Sima fusion construct, the *EGFP* coding sequence was amplified from a p*EGFP-C1* plasmid (Clontech Laboratories, Inc.) with primers including SacII restriction sites on their 5′ ends and cloned in frame in a SacII site that was previously inserted by PCR upstream of Sima coding sequence in a pGEM-T Easy vector (Promega). EGFP-Sima was finally subcloned into XbaI-NotI sites of a pMT/Bip/V5-His vector. Except for Sima.mNES3-4, all Sima mutant constructs for transgenic line generation were engineered in a pMT-EGFP*Sima* plasmid and then subcloned into the pCaSpeR-UAS vector as EcoRI-NotI fragments (see below). Sima ΔHLH was obtained by NruI partial digestion of pMT-EGFP*Sima* and subsequent religation. This resulted in the deletion of 141 nucleotides encompassing amino acids 78 to 124. Sima.mNES1-4, SimaF92Y, SimaL101A, SimaM114A, and SimaI123A were generated by overlap extension PCR to obtain fragments bearing the point mutations depicted in Fig. 6A and 7A, below. Amplification products for Sima.mNES3-4 were digested with BamHI, and the resulting 842-bp fragment was replaced in wild-type pCaSpeR-UAS Sima. All other PCR products were digested with BglII, and the 706-bp fragment was replaced in wild-type pMT-EGFP*Sima*. The mutations were confirmed by automatic sequencing.

EGFP-NES and EGFP constructs encoded in the pMT/Bip/V5-His vector for S2 cell transfections were previously described (45). EGFP-SimaHLH, EGFP-CycleHLH, EGFP-TrhHLH, EGFP-DysHLH, EGFP-SimHLH, EGFP-TgoHLH, and EGFP-ClkHLH constructs were generated by in-frame cloning of sequences amplified by PCR into XbaI-NotI sites of the pMT/Bip/V5-His-EGFP plasmid. The HRE-Luc construct that was used for Sima-dependent transcription assays in S2 cells was previously described (12). Tgo and HA-Sima sequences to be expressed in mammalian COS-7 cells were cloned in the pcDNA6/V5-His vector (Invitrogen) using XbaI-NotI and EcoRI-NotI, respectively.

Structural modeling. The PredictProtein, Jpred, and PSIPRED servers (11, 44, 23) were used for secondary structure predictions. Mutations that preserved the overall secondary structure of α-helices, while impairing nuclear export activity, were designed using the Agadir prediction program (30) based on the helix/coil transition theory that considers specific interactions occurring in helices devoid of tertiary interactions.

Luciferase activity. For Sima transcriptional activity assays, plasmids encoding the wild type or mutated variants of Sima were cotransfected in S2 cells along with the HRE-luciferase reporter plasmid and with a pAc5.1/LacZ plasmid to normalize transfection efficiency. Forty-eight hours after transfections, cells were exposed to desferrioxamine (DFO) and expression of the encoded proteins was induced by addition of 0.4 mM $CuSO_4$ for 24 h. One day later, cells were harvested and lysed, and luciferase and β-galactosidase activities were assayed. Luciferase activity was determined by using the Steady-Glo reagent (Promega), following the instructions of the manufacturer.

S2 cell transfections and analysis of subcellular localization of EGFP fusion constructs. All expression constructs were cloned in a pMT/Bip/V5-His plasmid (Invitrogen). Experiments using EGFP-Sima and EGFP-SimaΔHLH constructs were carried out in stable cell lines. Expression of the chimeras was induced by addition of 0.4 mM $CuSO_4$ for 6 to 8 h, after which cells were then observed with a confocal microscope (LSM5; Carl Zeiss, Pascal). Hypoxic treatments were carried out by exposing cells to 1% O_2 during 8 h in a Forma Scientific 3131 incubator. Leptomycin B (LMB; Sigma-Aldrich) was added at a 30 nM final concentration, and results were immediately analyzed in the confocal microscope; cell nuclei were visualized by Hoechst 33342 staining. For scoring subcellular localization, cells were classified into three categories: nuclear, for cells in which nuclear fluorescence was higher than cytoplasmic fluorescence; ubiquitous, for cells with an equal distribution of fluorescence between the nucleus and the cytoplasm; and cytoplasmic, for cells in which fluorescence in the cytoplasm was higher than in the nucleus. A total of 300 to 400 cells were analyzed for distribution of fluorescence, the proportion of cells assigned to each category was calculated, and category distributions were compared through a chi-square test.

Subcellular distributions of EGFP-HLH chimeras corresponding to Single minded, Dysfusion, Clock, and Trachealess were analyzed in transient cell transfections. Five μg of DNA was transfected with a calcium phosphate transfection kit (Invitrogen), and 24 h later, expression was induced by addition of 0.4 mM $CuSO_4$ for 6 to 8 h; cells were then observed with a confocal microscope (LSM5; Carl Zeiss, Pascal). Analysis of subcellular localization of the chimeras was carried out with the confocal microscope by measuring the intensity of EGFP fluorescence per μm^2 in the nucleus (N) and in the cytoplasm (C), followed by calculation of the N/C ratio.

Fly stocks and analysis of Sima subcellular localization in vivo. Transgenic lines were generated by P-element germ line transformation using standard procedures. UAS-sima and LDH-LacZ lines have been previously described (31). Analysis of Sima subcellular localization in vivo was performed in transgenic embryos overexpressing the Sima wild-type protein or altered variants of Sima under control of an en-Gal4 driver. To obtain synchronized embryos, egg-laying agar plates were replaced every 3 h, and embryos were grown at 25°C in normoxia until the desired stage and then transferred to hypoxia for 4 h. Hypoxic treatments were applied in a Forma Scientific 3131 incubator at 25°C; embryos were then recovered, fixed, and immunostained with anti-Sima antibodies (1, 31). Observations were performed with an Olympus BX60 microscope or a Carl Zeiss LSM5 Pa confocal microscope. Quantitative analyses of subcellular localization were carried out as previously described (12). Briefly, each embryo was classified into one of three categories of Sima subcellular localization: cytoplasmic, where more than 90% of the cells in the Engrailed-expressing stripes showed cytoplasmic localization; nuclear, where more than 90% of the cells in the Engrailed-expressing stripes had nuclear localization; and ubiquitous, where less than 90% of the cells had cytoplasmic or nuclear localization. The percentage of embryos assigned to each subcellular localization category was calculated,

and category distributions in the different genotypes were compared with a chi-square test.

Yeast two-hybrid interaction assays. For examining protein-protein interactions we have used the LexA *Saccharomyces cerevisiae* two-hybrid interaction system (35a). Wild-type Sima or mutated Sima amino acids (aa) 32 to 494, including the bHLH and PAS domains, were used as baits by cloning them into the pEG202 vector, which fuses the sequence to be tested onto a LexA DNA binding domain. Tgo full-length protein (644 aa) was used as a prey by cloning it into a pJG4-5 plasmid. The reciprocal experiment using Tgo bait could not be performed because the reporter was activated in the absence of a prey (47). Bait plasmids were transformed into the yeast strain EGY42, and prey plasmid was transformed into the EGY48 strain, which contains the pSH18-34*lacZ* reporter gene preceded by eight LexA binding sites. The interaction assays were performed in diploid yeast cells generated by mating the corresponding haploid strains. At least three independent colonies were selected for each bait-prey pair and assayed for β-galactosidase activity in liquid culture assays, using *o*-nitrophenyl-β-D-galactoside as a substrate, with glucose or galactose as a carbon source.

Coimmunoprecipitation assays. pcDNA6/V5-His plasmids encoding HA-Sima and Tango were transiently transfected by using a calcium phosphate transfection kit (Invitrogen) in COS-7 cells grown in Dulbecco's modified Eagle's medium (Invitrogen) supplemented with 10% heat-inactivated fetal calf serum; 48 h later cell extracts were prepared as previously described (12a) in buffer C containing 0.5 mM dithiothreitol and a protease inhibitor cocktail (Sigma). For immunoprecipitation assays, 200 μg of extract was incubated for 1 h with anti-hemagglutinin (anti-HA) antibody (Santa Cruz) in 20 mM Tris-HCl (pH 7.5), 120 mM NaCl, 1% Triton, and 10% glycerol in a final volume of 1 ml. Then, 30 μl of 50% protein G-Sepharose was added to the reaction mixture and the mixture was incubated for 12 h at 4°C under rotation. After rapid centrifugation, Sepharose beads were washed three times with buffer (20 mM Tris-HCl [pH 7.5], 120 mM NaCl, 1% Triton, and 10% glycerol) and then boiled in protein sample buffer, and proteins were resolved by sodium dodecyl sulfate-polyacrylamide gel electrophoresis followed by immunoblotting using anti-Tgo antibodies (Developmental Studies Hybridoma Bank) diluted 1:1,000.

RESULTS

Identification of a functional nuclear localization signal next to the Sima C terminus. Proteins with a molecular mass larger than 60 kDa require NLSs in order to be targeted to the nucleus through the nuclear pore complex (27). Canonical NLSs consist of two classes: monopartite NLSs, composed of a single stretch of basic amino acids (24), and bipartite NLSs, consisting of two basic residues, a spacer of approximately 10 amino acids, and a second region consisting of at least three basic residues out of five residues (43). Inspection of the Sima amino acid sequence revealed the occurrence of two candidate atypical bipartite nuclear localization signals: NLS1 (aa 537 to 568) and NLS2 (aa 1210 to 1229), both of them with longer-than-normal spacers between the two stretches of basic amino acids, and a monopartite candidate nuclear localization signal, NLS3, spanning amino acids 1406 to 1409 (Fig. 1A and B). To examine whether these predicted Sima nuclear localization signals were functional, we conducted a structure-function analysis by expressing in transgenic embryos in hypoxia (5% O_2) either full-length Sima (wild type) (Fig. 1C) or deleted forms of the protein (Fig. 1D to F), followed by analysis of their subcellular localizations. As reported in our previous studies (12, 31), we utilized the *Drosophila* Gal4/upstream activation sequence (UAS) overexpression system in transgenic lines (5) to override the rapid rate of protein degradation and to be able to analyze Sima localization. Full-length Sima protein was mostly cytoplasmic in normoxia and accumulated in the nuclear compartment upon hypoxic exposure (12, 31) (Fig. 1C). To identify Sima functional NLSs, we initially deleted the C-terminal portion of the protein, starting at residue 971, to generate SimaΔ971-1507, which lacks candidates NLS2 and NLS3. As shown in Fig. 1D, this deletion provoked accumulation of Sima exclusively in the cytoplasm even in hypoxia, suggesting that either NLS2 or NLS3 is critically required for Sima nuclear import. Next, we generated a smaller C-terminal deletion encompassing residues 1252 to 1507 (Fig. 1E), which included candidate NLS3 but not NLS2. This deleted form of Sima exhibited nuclear localization in hypoxia (Fig. 1E) and cytoplasmic localization in normoxia (not shown), indicating that the putative NLS3 is not required for nuclear import. In contrast, specific deletion of NLS2 (SimaΔ1210-1229) totally prevented Sima nuclear import (Fig. 1F), suggesting that it is likely a functional NLS. Remarkably, the NLS2 sequence has significant amino acid identity with bipartite nuclear localization signals previously described in mammalian HIF-α subunits (32) (Fig. 1G).

To further demonstrate that NLS2 is indeed a functional nuclear localization signal, we explored the ability of the sequence spanning amino acids 1210 to 1229 to drive nuclear localization of an EGFP reporter in *Drosophila* Schneider (S2) cells. Whereas subcellular localization of an EGFP control element lacking an NLS was essentially ubiquitous (slightly nuclear) in the S2 cells (Fig. 2A and G), an EGFP positive control construct, bearing an NLS derived from the simian virus 40 large T antigen, was clearly more nuclear (Fig. 2B and G). When we tested the candidate NLS2 by the same method, we found that nuclear localization of the EGFP reporter was dramatically enhanced (Fig. 1C and G), suggesting that Sima NLS2 is a strong functional nuclear localization signal. In order to determine whether the two stretches of basic amino acids separated by 14 residues in NLS2 are both required for nuclear import activity, we introduced point mutations as depicted in Fig. 2D to F. Replacement of a single residue in each of the two stretches of basic amino acids, or in both stretches simultaneously, provoked complete destruction of NLS2 nuclear import activity (Fig. 2D to G). In all three cases the EGFP reporter exhibited a subcellular localization that was indistinguishable from that of the EGFP control construct (Fig. 2A and G). Taken together, the above results strongly suggest that NLS2 is an atypical bipartite nuclear localization signal with a 14-amino-acid spacer and that this NLS is necessary and sufficient to drive Sima nuclear import. In order to address the possibility that NLS2-dependent nuclear import might be influenced by oxygen tension, we examined subcellular localization of the EGFP-NLS2 chimera in transfected S2 cells upon exposure to 1% O_2 for 24 h. Localization of the chimeric protein under these conditions mimicked the localization observed in normoxia (data not shown).

Sima shuttles continuously between the nucleus and the cytoplasm. It has been proposed that in normoxia HIF-α resides in the cytoplasm and upon a hypoxic stimulus it is imported into the nucleus (9, 25, 32). However, it is becoming increasingly evident that many proteins whose nucleo-cytoplasmic localization depends on external stimuli shuttle continuously between the nucleus and the cytoplasm (33, 51). Hence, we decided to analyze the possibility that Sima is a shuttling protein that varies its steady-state subcellular localization by modifying the import versus export rate, in an oxygen-dependent manner. If this were the case, interfering with its putative nuclear export would be expected to modify the steady-state

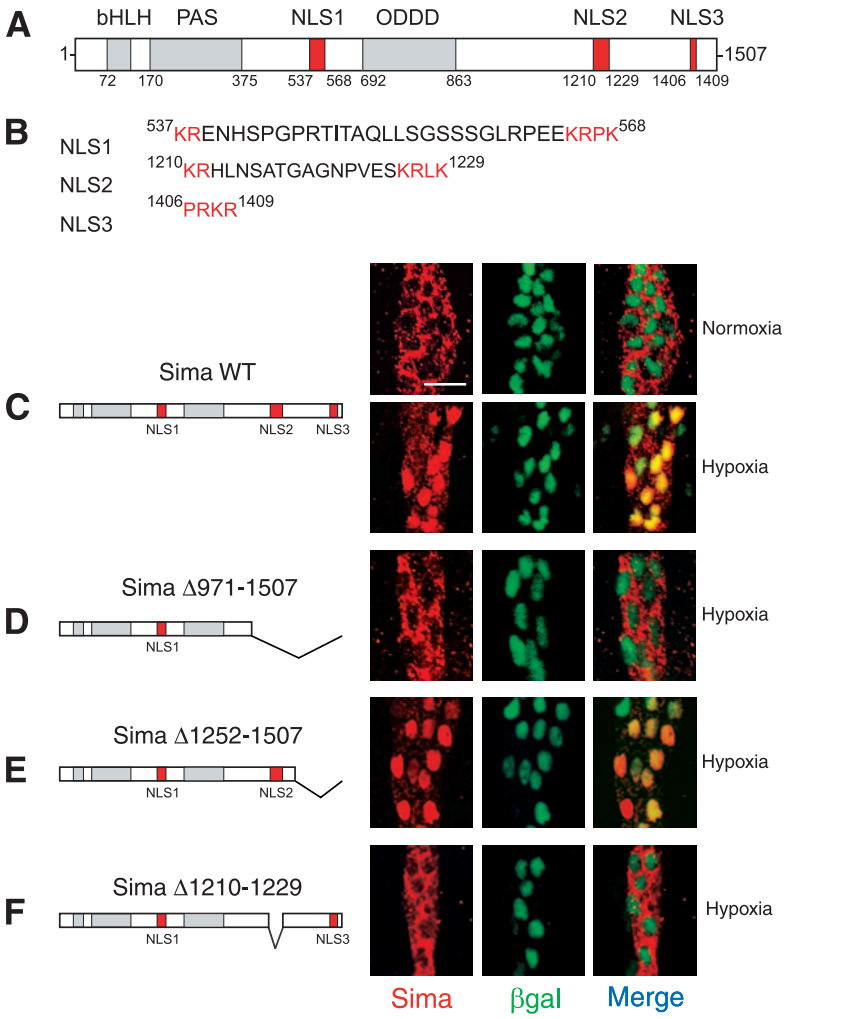

G

		Spacer length
Sima	1210KRHL...NSAT...GAG..NPVES.....KRLKG1230	14
HIF1a	720KRKMEHDGSLFQAVGIGTLLQQPDDHAATTSLSWKRVKG758	32
HIF2a	705KRQLEYEKQAFQDPSGGDPPGGS.....TSHLMWKRMKN738	27
HIF3a	561KRALAQSSEDK.....GLELLEIKPP.....KRSPR586	19

FIG. 1. Identification of a Sima functional NLS. (A) Schematic representation of the Sima protein. Candidates NLS1, NLS2, and NLS3 are shown in red. (B) Amino acid sequence of candidate Sima NLSs. NLS1 (aa 537 to 568) and NLS2 (aa 1210 to 1229) have atypical bipartite structures in which the separation between the two stretches of basic amino acids (in red) is longer than 10 residues. The NLS3 (aa 1406 to 1409) PRKR sequence matches a typical monopartite NLS consensus. (C to F) Subcellular localization of full-length (C) or deleted (D to F) forms of Sima. Sima constructs were expressed in UAS transgenic embryos under control of an *en-Gal4* driver, and subcellular localization was analyzed with an anti-Sima antibody (red). The embryos also contained a UAS-nGFP.LacZ element that included a nuclear localization signal and, thus, β-galactosidase expression (green) marked the nuclei. Cells from one of the Engrailed stripes are shown in the photographs. (C) Full-length Sima was predominantly cytoplasmic in normoxia (21% O_2) and mainly nuclear in hypoxia (5% O_2). WT, wild type. (D) SimaΔ971-1507 that lacked candidates NLS2 and NLS3 failed to enter the nucleus in hypoxia and therefore was detected only in the cytoplasm. (E) SimaΔ1252-1507, lacking NLS3, behaved exactly as full-length Sima and could be detected in the nucleus in hypoxia. (F) SimaΔ1210-1229 failed to enter the nucleus in hypoxia, indicating that NLS2 is a functional nuclear localization signal, necessary for Sima nuclear import. Bar, 10 μm. (G) Sequence alignment between nuclear localization signals of Sima and human HIF-α subunits. Note that the two blocks of basic residues in the bipartite NLSs are highly conserved, whereas the length of the spacer varies considerably between the different HIF-α subunits.

subcellular localization by increasing the proportion of the protein localized in the nucleus. In eukaryotic cells, nuclear export of many proteins is mediated by the nuclear export receptor CRM1, which binds NESs on cargo proteins, thereby recruiting them to the Ran ternary protein export complex that transverses the nuclear pore (15, 33, 48).

CRM1 is specifically inhibited by LMB, a metabolite produced by *Streptomyces* spp. that prevents the formation of the

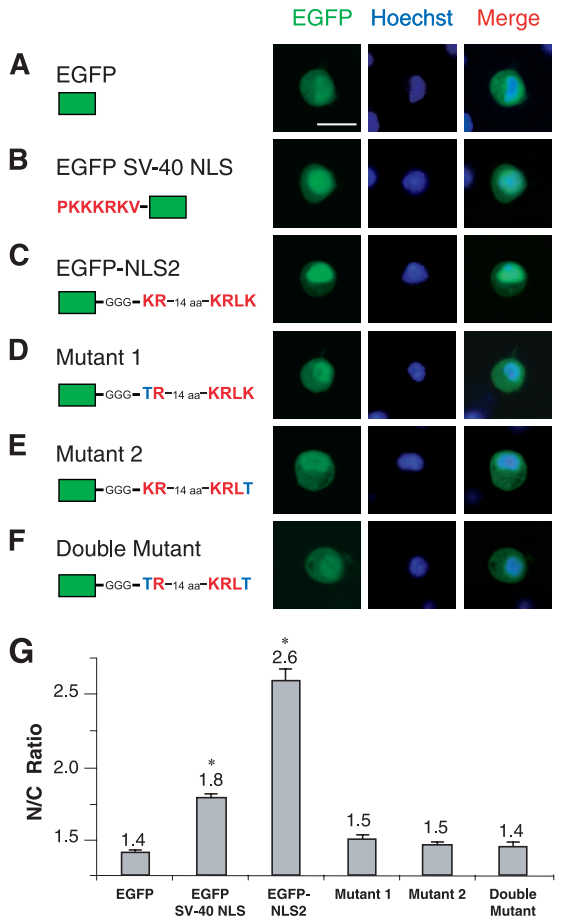

FIG. 2. NLS2 is an atypical bipartite nuclear localization signal that can drive nuclear import of an EGFP reporter in *Drosophila* Schneider (S2) cells. S2 cells were transfected with different EGFP constructs (A to F) and then subcellular localization was assessed with a confocal microscope by comparing fluorescence intensity in the nuclei (that were marked by Hoechst staining) with fluorescence intensity in the cytoplasm. (G) The N/C fluorescence ratio was calculated for each construct and compared with the N/C ratio of an EGFP control construct (A) through a Student *t* test. *, significantly different. The EGFP simian virus 40 (SV-40) NLS positive control (B) and EGFP-NLS2 (C) were clearly more nuclear than EGFP (G) ($P < 10^{-14}$; $n > 16$). Single amino acid replacements in any of the two stretches of basic residues in NLS2 (D and E) or in both stretches simultaneously (F) totally destroyed NLS2 nuclear import activity (G). Mutated amino acids are shown in blue. Bar, 10 μm.

CRM1-Ran-Cargo ternary complex (28). We therefore investigated whether Sima steady-state subcellular localization was dependent on CRM1 by addressing if it was influenced by LMB. To this end, we set up a cell culture system that enabled pharmacological intervention. We engineered an EGFP-Sima chimera in a pMT plasmid (metallothionein promoter) that was transiently transfected into *Drosophila* Schneider (S2) cells, and the resulting subcellular localization was analyzed by fluorescence microscopy. For scoring subcellular localization, cells were classified into three categories, namely, cytoplasmic, ubiquitous, and nuclear (Fig. 3B). As depicted in Fig. 3C, the proportion of cells exhibiting nuclear localization of EGFP-Sima was threefold higher in hypoxia (3% O_2) than in normoxia, paralleling Sima regulation by oxygen in living embryos (12). DFO or LMB treatment in normoxia provoked an effect very similar to that of observed upon exposure to hypoxia (Fig. 3C). These results suggest that Sima is a shuttling protein and that nuclear export is mediated at least in part by CRM1.

Occurrence of CRM1-dependent nuclear export signals in the bHLH domain of Sima. To begin characterizing Sima nuclear export, we searched the primary sequence for consensus CRM1-dependent NESs by using the NES Finder 0.2 software (6). As shown in Fig. 3A, four predicted consensus NESs occur in the Sima sequence. Remarkably, two of these NESs that map in the bHLH domain have been conserved in most HIF-α proteins throughout evolution (Fig. 3E), suggesting that they are likely relevant for HIF function. It has been reported that nuclear export signals tend to adopt an α-helical structure (29). According to the predicted structure of the Sima bHLH domain (6, 36), one of these NESs (NES1), which encompasses amino acids 92 to 101 and exhibits a 2-3-1 type of CRM1-dependent consensus, is localized at the first helix of the bHLH domain (Fig. 3D and E). The second putative NES (NES2) has a typical 3-2-1 NES consensus and maps to the second helix extending between residues 115 and 124 (Fig. 3D and E). The bHLH is probably the domain with the highest degree of evolutionary conservation in the bHLH-PAS family, displaying a stereotypical array of two amphipathic helices separated by a loop. However, not all the residues within the domain are equally conserved among HIF-1α homologues. A remarkable degree of amino acid identity is observed in three particular stretches of amino acids: (i) at the basic region where physical contact with the DNA takes place; (ii) in a stretch with the sequence LDKAS at the beginning of helix 2; (iii) in the residues that constitute NES1 and NES2 (Fig. 3E). This remarkable conservation of the presumptive NESs prompted us to initiate functional studies to test if they indeed participate in nuclear export. We began by analyzing in transfected S2 cells the subcellular localization of an EGFP-Sima fusion protein in which the entire HLH motif was deleted (EGFP-SimaΔHLH). As depicted in Fig. 3F, this deleted version of Sima was remarkably more nuclear than wild-type Sima, and its subcellular localization was unaffected by LMB (Fig. 3F; compare with C), suggesting that these candidate NESs might play a role in Sima nuclear export.

In order to answer if the behavior of the EGFP-SimaΔHLH chimeric protein in S2 cells is paralleled by its behavior in *Drosophila* living embryos, we generated transgenic lines expressing SimaΔHLH under control of a UAS promoter, as described above. When expressed through an *en-Gal4* driver, SimaΔHLH was clearly more nuclear than full-length Sima, and this could be verified at different oxygen concentrations all throughout embryogenesis, as revealed by anti-Sima immunofluorescence (Fig. 4A and B).

Having established that the bHLH domain is necessary for normal regulation of Sima steady-state subcellular localization, we looked for direct evidence that this domain is specifically required for nuclear export. To this end, we set up a reoxygenation assay in which embryos expressing Sima were exposed to 1% O_2 for 4 h, transferred to normoxic conditions, and fixed at different times after reoxygenation; Sima subcellular localization was then analyzed by immunofluorescence. At 1% O_2, Sima was totally nuclear and exported from the nucleus to the cytoplasm only 10 min after reoxygenation (Fig. 4C). By using

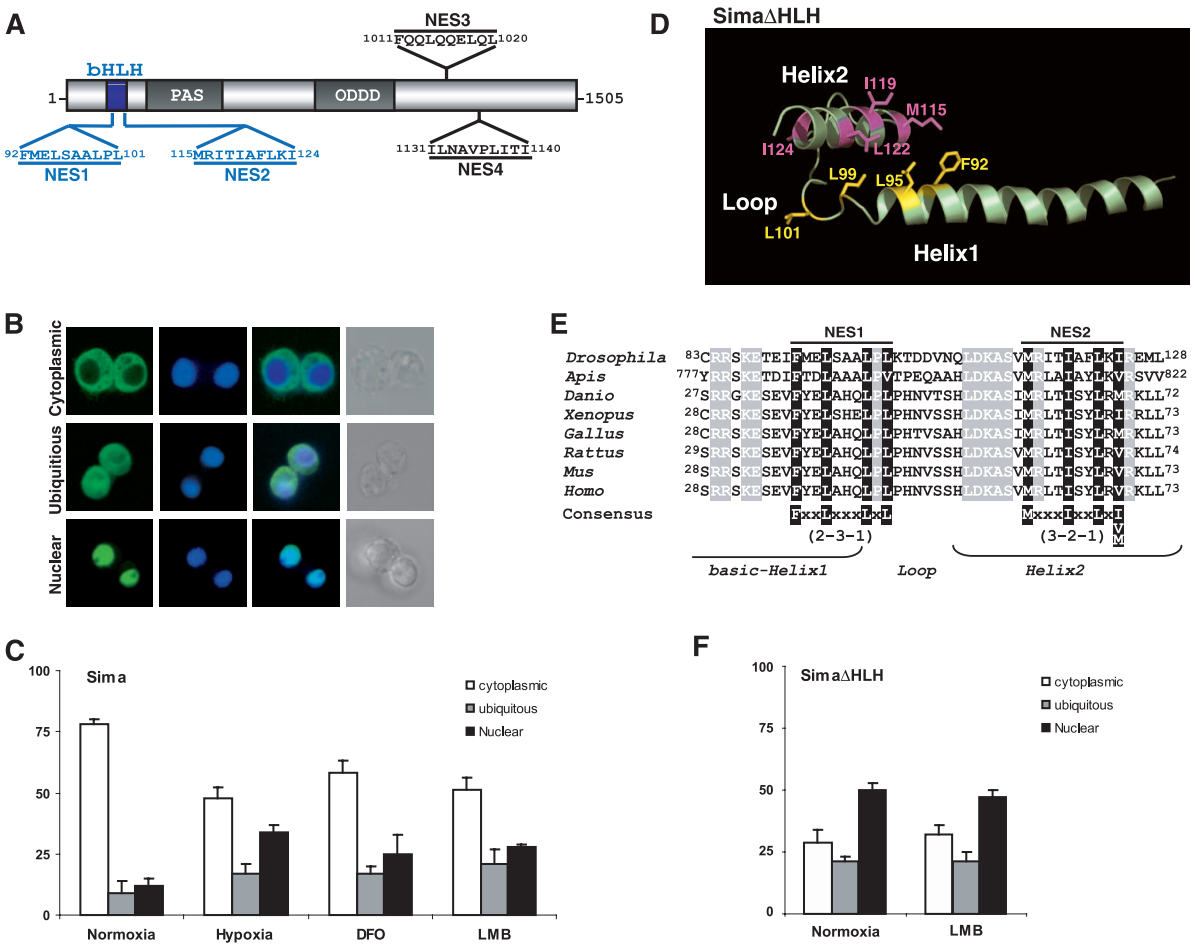

FIG. 3. Subcellular localization of Sima responds to hypoxia or DFO and is sensitive to LMB. (A) Schematic representation of the Sima protein, showing the bHLH, PAS, and ODDD. The bHLH domain is marked in blue. The positions and sequences of four putative CRM1-dependent nuclear export signals (NES1 to -4) are shown. (B) An EGFP-Sima fusion protein was transiently transfected in S2 cells, and subcellular localization was analyzed under a fluorescence microscope. Based on the subcellular localization of the chimeras, the cells were classified into three categories: nuclear, ubiquitous, and nuclear. (C) Distribution of the cells in the three categories as defined for panel B maintained in normoxia (21% O_2), exposed to hypoxia (1% O_2), or in normoxia after adding 150 μm DFO or 30 nM LMB. Sima subcellular localization becomes more nuclear in hypoxia or upon addition of DFO or LMB (chi-square test, $P < 10^{-2}$; $n > 300$). (D) Three-dimensional model of the bHLH domain of Sima. The hydrophobic amino acids that define the CRM1 binding consensus are shown in color. (E) Amino acid sequence of the bHLH domain of HIF-1α proteins from different phyla, ranging from *Drosophila* to humans. The conserved NES1 and NES2 consensus sequences are highlighted with black boxes; other conserved residues of the bHLH domain are marked with gray boxes. (F) An EGFP-SimaΔHLH fusion protein was transiently transfected in S2 cells, and the distribution of categories of subcellular localization was analyzed in normoxia as for panel C with or without the addition of LMB. The mutated Sima variant loses sensitivity to LMB.

the same strategy, we studied the behavior of SimaΔHLH; in contrast to full-length Sima, nuclear export of the deleted form was remarkably slower (Fig. 4D), suggesting that the HLH motif plays a central role in oxygen-dependent nuclear export of the protein. Of note, it is still possible that nuclear export impairment of SimaΔHLH is not directly due to deletion of specific functional NESs but, rather, could be an indirect effect derived from inefficient heterodimerization with the β-subunit (see below).

Characterization of Sima CRM1-dependent nuclear export signals. To begin examining whether these NESs might be functional, we tested if the HLH sequence had the capacity to direct nuclear export of a reporter in an autonomous manner. We fused the HLH region of the bHLH domain of Sima (amino acids 77 to 130) to EGFP (EGFP-SimaHLH) and studied its subcellular localization in transfected S2 cells, along with the localization of two control constructs, EGFP alone and EGFP fused to an NES derived from the protein kinase A inhibitor (45, 52). As shown in Fig. 4E and H, EGFP-SimaHLH was largely excluded from the nuclear compartment, displaying a subcellular distribution very similar to that of the EGFP-NES positive control (Fig. 4E and G); upon addition of LMB, the localization of EGFP-SimaHLH and EGFP-NES became remarkably more nuclear (Fig. 4E, G, and H), indicating that both constructs are subjected to active CRM1-dependent nuclear export. As expected, subcellular localization of EGFP alone was unaffected by LMB, which exhibited a ubiquitous (though slightly nuclear) localization (Fig. 4E and F). These results suggest that the bHLH domain of Sima includes at least one functional NES.

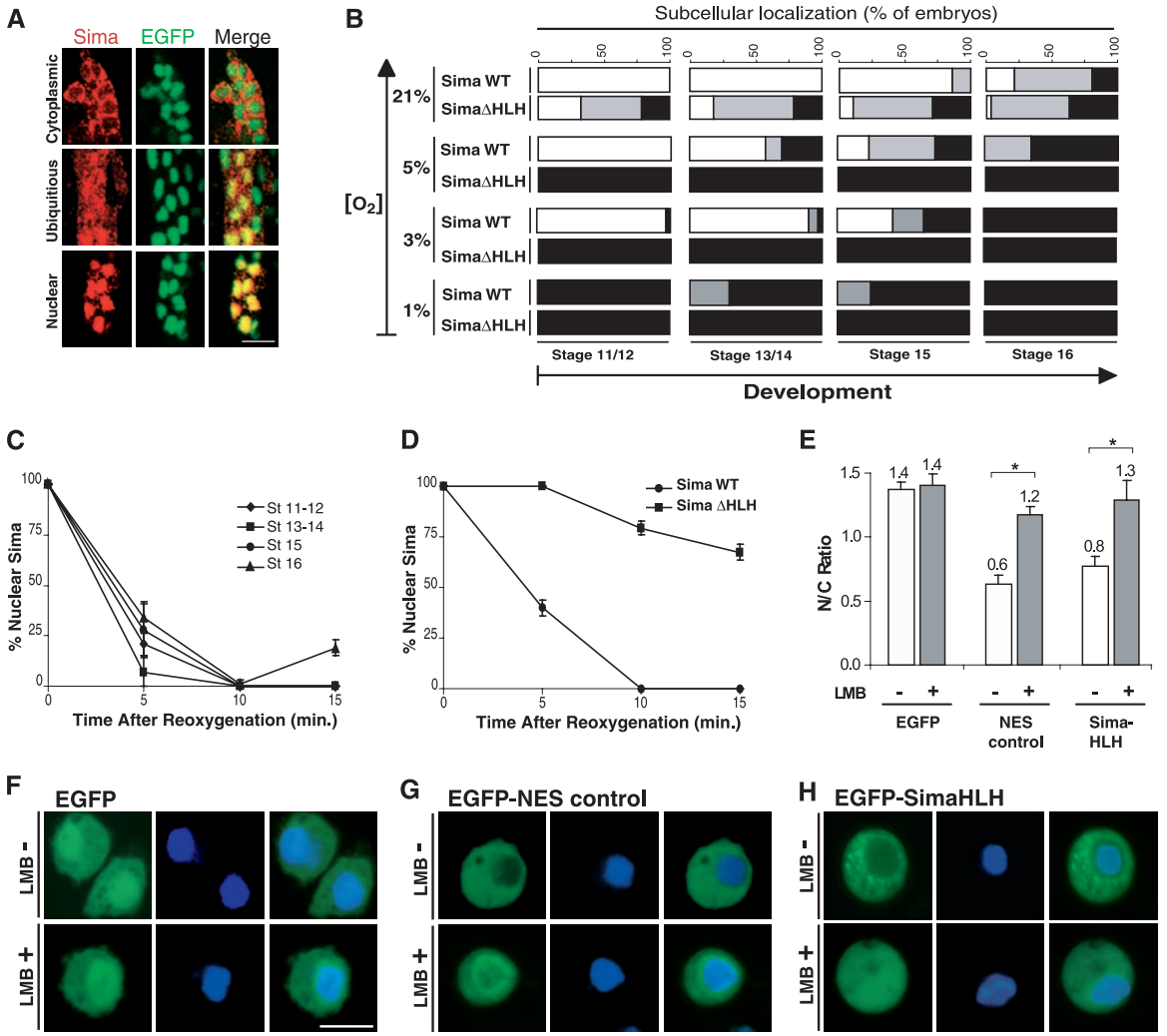

FIG. 4. (A) Definition of three categories of Sima subcellular localization. Sima and a β-galactosidase (β-gal) variant bearing a nuclear localization signal were simultaneously expressed in UAS transgenic embryos under control of an *engrailed-Gal4* driver and visualized by immunofluorescence. Three arbitrary categories of subcellular localization were defined: cytoplasmic, where more than 90% of the cells in the embryo exhibited cytoplasmic localization; nuclear, where more than 90% of the cells showed nuclear localization; ubiquitous, where less than 90% of the cells showed cytoplasmic or nuclear localization. Bar, 10 μm. (B) Quantitative analysis of subcellular localization of Sima wild type and SimaΔHLH in *en-Gal4/UAS-Sima* transgenic embryos at different oxygen concentrations throughout embryogenesis was performed as previously described (12). White, cytoplasmic localization; black, nuclear localization; gray, ubiquitous localization. Sima subcellular localization in wild-type embryos was progressively more nuclear as embryogenesis proceeded and gradually more nuclear as oxygen levels decreased (chi-square test, $P < 10^{-2}$; $n > 30$). Nuclear localization was increased in SimaΔHLH embryos ($P < 10^{-2}$; $n > 30$) at 21%, 5%, and 3% O_2 concentrations. At 1% O_2 Sima was almost totally nuclear in wild-type embryos throughout development. (C) At all embryonic stages, Sima is totally exported from the nucleus in only 10 min after reoxygenation. Embryos were exposed to 1% O_2 during 4 h, and then they were transferred to normoxia and stained for Sima at different time points after reoxygenation. Time course variation of the proportion of Sima protein localized in the nucleus of embryos from different stages expressing wild-type Sima. (D) Time course variation of the proportion of SimaΔHLH or wild-type Sima protein localized in the nucleus in stage 15 embryos. The experimental procedure described for panel C was followed. SimaΔHLH nuclear export after reoxygenation was severely impaired (Kaplan-Meier, $P < 10^{-4}$; $n > 30$). (E to H) EGFP control constructs or an EGFP-SimaHLH fusion was transiently transfected in S2 cells; 6 h after induction with $CuSO_4$, cells were treated or not with 30 nM LMB and, 2 h later, subcellular localization was analyzed with a confocal microscope. Bar, 10 μm. (E) At least 10 cells from each construct and condition were quantitatively analyzed by measuring the intensity of EGFP fluorescence per μm^2 in the nucleus (N) and cytoplasm (C); the N/C ratio is represented. *, $P < 10^{-4}$, Student's *t* test; $n > 10$).

Given the multiple functions of the bHLH domain, it is important to address directly a possible role of the candidate individual NES mapping in this motif. Thus, we sought to analyze the functionality of NES1 and NES2 in the context of the full-length Sima protein in transgenic embryos as above. Mutagenesis of two out of four hydrophobic amino acids of the CRM1 consensus in nuclear export signals is known to cripple NES function (2, 18, 29, 35). Since NES1 and NES2 are conserved among many bHLH-PAS proteins, we sought to mutagenize those amino acids that display the highest conservation, namely, the second and third hydrophobic residues of the consensus. Thus, we generated UAS-transgenic lines bearing

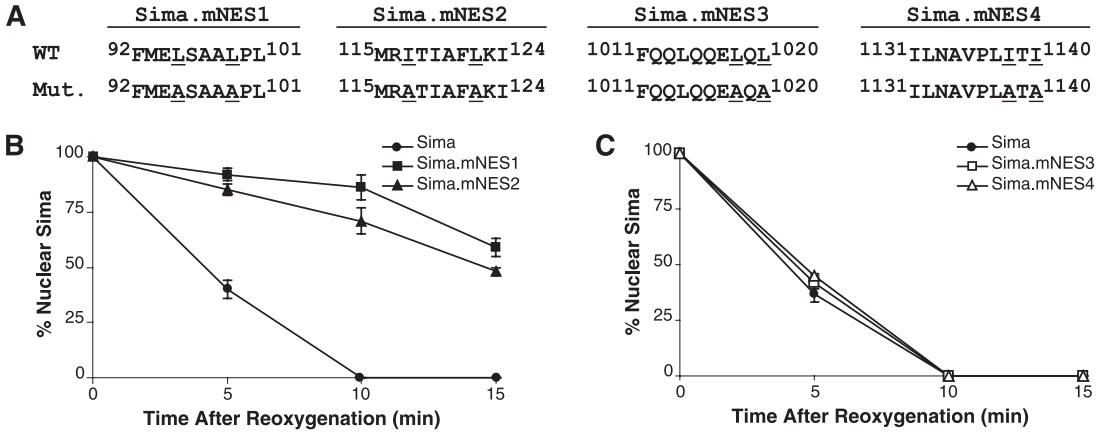

FIG. 5. Mutagenesis of NES1 or NES2 at the Sima bHLH domain provokes a severe impairment of Sima nuclear export in transgenic embryos after reoxygenation. (A) UAS-Sima transgenic lines were generated by P-element germ line transformation of wild-type or altered variants of Sima in which NES1 to -4 were mutated (mutagenized residues are underlined). (B and C) Embryos were exposed to 1% O_2 for 4 h, and then they were transferred to normoxia and stained for Sima at different time points after reoxygenation. Time course variation of the proportion of Sima protein localized in the nucleus of stage 15 embryos expressing wild-type Sima or Sima variants with mutations in the NES1/NES2 (B) reveals that these NESs are necessary for export ($P < 10^{-4}$, Kaplan-Meier; $n > 30$). The NES3 or NES4 mutation does not impinge on nuclear export (C).

mutated variants of Sima full-length protein, in which these hydrophobic residues of NES1 and -2 were replaced by alanines (Sima.mNES1 and Sima.mNES2) (Fig. 5A). As above, nuclear export of the Sima mutated variants was evaluated by assessing subcellular localization at different times after reoxygenation of the transgenic embryos (Fig. 4C and D). Nuclear export of Sima.mNES1 and Sima.mNES2 was severely impaired compared to wild-type Sima (Fig. 5B), suggesting that the two NESs mapping in the bHLH domain are required for Sima nuclear export. Because nuclear export of SimaΔHLH as well as that of the two NES-specific mutated variants was slowed but not completely abrogated (Fig. 4D), we examined whether any of the two other predicted CRM1-dependent export signals, NES3 and NES4, both of them mapping outside the bHLH domain (Fig. 3A), contribute to Sima nuclear export. We therefore generated Sima.mNES3 and Sima.mNES4 mutated variants, in this case, by replacing the third and fourth hydrophobic residues of the CRM1 binding consensus (Fig. 5A). The kinetics of nuclear export of Sima.mNES3 and Sima.mNES4 was analyzed in transgenic embryos upon reoxygenation as above, revealing that these candidate NESs do not contribute to nuclear export at all (Fig. 5C). These results indicate that NES1 and NES2 are both bona fide CRM1-dependent export signals that contribute to nuclear export of Sima wild-type protein in vivo and that NES3 and NES4 are not functional export signals.

Role of NES1 and NES2 in the regulation of Sima activity. The fact that Sima shuttles continuously between the nucleus and the cytoplasm raises the possibility that oxygen-dependent nuclear export is a physiological mechanism that contributes to the regulation of Sima transcriptional activity. The bHLH domain of Sima is critically involved in DNA binding as well as in heterodimerization with the β-subunit Tango. Hence, in order to test whether nuclear export is a mechanism that contributes to Sima regulation, we designed a new set of mutations that were expected to preserve the overall secondary structure of the α-helices 1 and 2 in the bHLH domain, while impairing nuclear export activity (see Materials and Methods). In each of these Sima mutant variants, one out of the four hydrophobic residues of the CRM1 binding consensus of either NES1 (SimaF92Y or SimaL101A) or NES2 (SimaM115A or SimaI124A) was mutagenized (Fig. 6A). Given that the HLH region is probably the most important dimerization interface with the β-subunit, we sought to examine whether the mutations affect heterodimerization with Tango by using a yeast two-hybrid system. As previously reported (47), the Tango full-length protein was used as a prey and amino acids 32 to 494 of Sima or Sima mutant variants were used as baits. As depicted in Fig. 6B and C, L101A and M115A Sima mutations displayed β-galactosidase activation levels comparable to wild-type Sima, indicating that the mutations do not interfere with Sima-Tango physical interactions. Coimmunoprecipitation experiments further confirmed that Sima-Tango physical interactions are not disrupted in SimaL101A or SimaM115A mutant variants (Fig. 6D).

In order to examine the intrinsic transcriptional activity of these new mutations, plasmids encoding mutant or wild-type Sima versions were cotransfected into S2 cells, along with a Sima-responsive luciferase transcriptional reporter (12), and the transfected cultures were exposed to the iron chelator DFO, a chemical agent known to mimic hypoxia (Fig. 3C). The mutations SimaF92Y and SimaI124A both induced the luciferase reporter to a similar extent as wild-type Sima, suggesting that the structure of α-helices was intact in both cases (Fig. 6E). However, SimaL101A and SimaM115A exhibited a 40 to 43% reduction of their intrinsic transcriptional activities, as revealed by the expression of the luciferase reporter (Fig. 6E).

Having established that the four Sima mutated variants were at least partially active, we studied if their nuclear export was impaired in UAS transgenic fly lines by following the experimental strategy described above. At least five transgenic lines were generated for each construct, and protein expression levels were assessed by anti-Sima immunofluorescence, in crosses with an *en-Gal4* driver line (data not shown). Based on comparable protein expression levels, one transgenic line of each construct was selected, and nuclear export upon reoxygenation

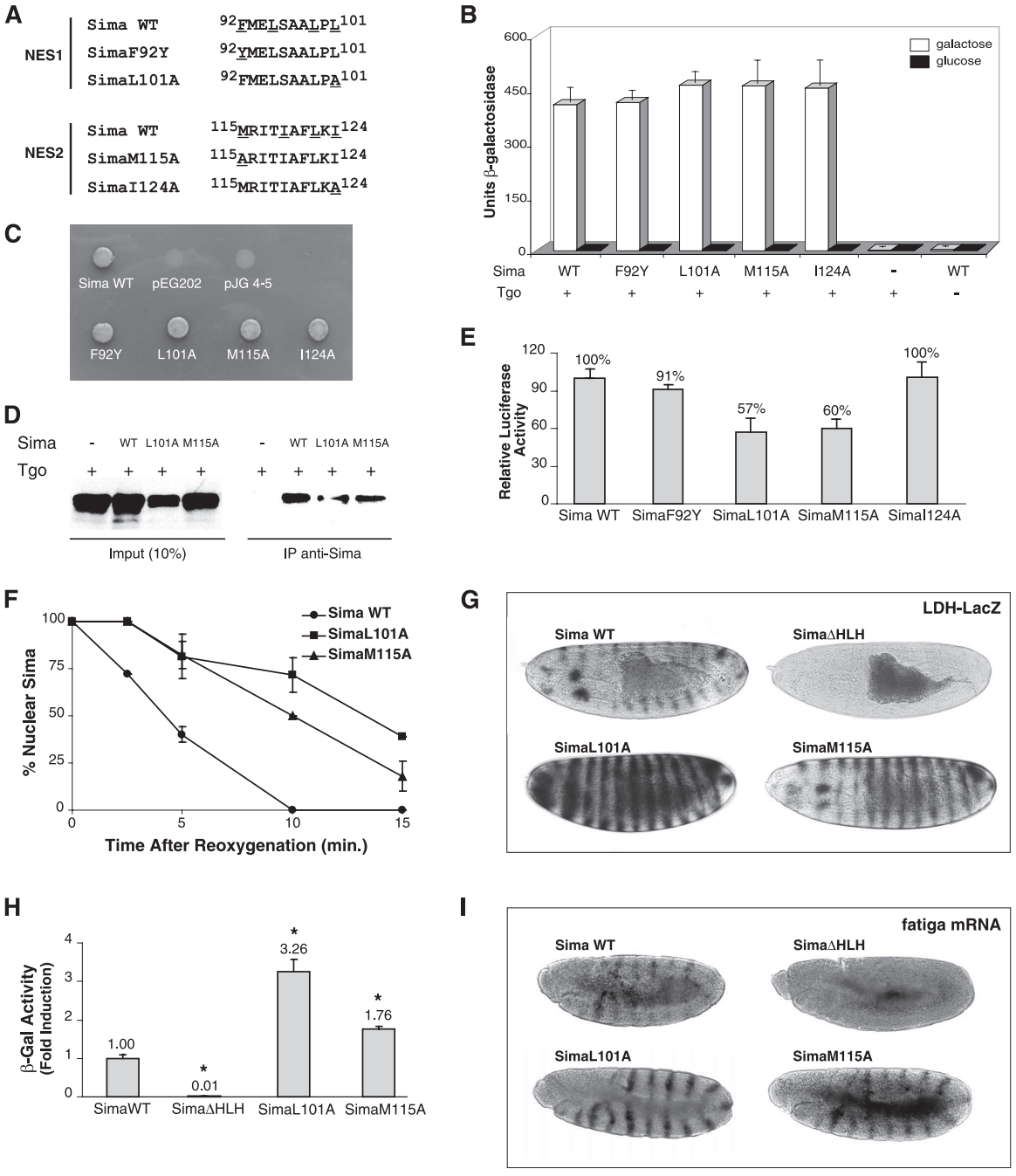

FIG. 6. Sima defects in nuclear export increase its transcriptional activity. (A) Amino acid sequence of the bHLH domain of Sima variants with mutations in NES1 or NES2. (B) Yeast two-hybrid assays showed that Tgo dimerizes with Sima. Yeast liquid cultures containing Sima as a bait and Tgo as a prey were assayed for β-galactosidase activity using glucose or galactose as a carbon source and employing the pSH18-34 *lacZ* gene as a reporter. The empty vectors pEG202 and pJG4-5 were used as negative controls. (C) Sima-Tango interactions in the two-hybrid system, revealed by the ability of galactose-induced cells to grow in a medium lacking leucine, revealing the specific interactions. Note that all interactions were positive; the only cells that failed to grow were the negative controls containing the pEG202 and pJG4-5 empty vectors. (D) Sima-Tango coimmunoprecipitation assays. HA-tagged wild type (WT) or mutated Sima variants were cotransfected with Tango in COS7 cells; extracts were subjected to immunoprecipitation with an anti-HA antibody, after which they were analyzed by Western blotting with an anti-Tango antibody. Note that Sima-Tango interactions were maintained in the mutagenized Sima variants. (E) Intrinsic transcriptional activities of SimaL101A and SimaM115A are reduced under conditions of constitutive transcriptional activation. S2 cells were cotransfected with wild type or mutagenized Sima variants, along with an LDH-luciferase reporter plasmid, 2 days later they were treated with 150 μM desferrioxamine for 20 h, and luciferase activity was assayed. (F) Poststimulus nuclear export of SimaL101A and SimaM115A is slower than export of wild-type Sima in transgenic embryos. Stage 15 *UAS* transgenic embryos expressing the wild type or mutagenized Sima variants through an *en-Gal4* driver were exposed to 1% O_2 for 4 h and then transferred to normoxia. The proportion of embryos with Sima protein localized in the nucleus was assessed by anti-Sima immunofluorescence at different time points after reoxygenation ($P < 10^{-4}$, Kaplan-Meier; $n > 30$). (G) A Sima-responsive LDH-LacZ transcriptional reporter was crossed into the UAS lines expressing the wild type or mutagenized Sima variants, and expression of the reporter was analyzed by 5-bromo-4-chloro-3-indolyl-β-D-galactopyranoside staining in normoxic embryos. (H) Expression of the LDH-LacZ reporter was quantitatively assessed in the embryos described for panel G by using the CPRG (chlorophenyl red-β-D-galactopyranoside)-based β-galactosidase activity colorimetric assay (*, $P < 10^{-3}$, Student's *t* test; $n = 3$). (I) Expression of the Sima target gene *fatiga* was studied in the embryos described for panel G by mRNA in situ hybridization.

of the transgenic embryos was analyzed. Whereas the mutations F92Y and I124A did not provoke a significant effect on the rate of nuclear export (data not shown), L101A and M115A clearly impaired Sima nuclear export (Fig. 6F). To analyze the role of nuclear export in the regulation of Sima transcriptional activity, a Sima-dependent LacZ transcriptional reporter (31) was crossed into the UAS lines expressing different Sima variants under control of an *en-Gal4* driver. As shown in Fig. 6G and H, induction of the reporter in L101A and M115A Sima lines was two- to three fold higher than in embryos expressing wild-type Sima. As expected, expression of the reporter in the line that lacked the entire bHLH domain (SimaΔHLH), which was used as a negative control, was below detection levels (Fig. 6G and H). These results strongly suggest that nuclear export plays a role in the regulation of Sima overall transcriptional activity. This notion is strengthened by the fact that, under conditions of Sima maximal activation in S2 cells (DFO), the intrinsic transcriptional activity of L101A and M115A Sima variants was lower than the activity of wild-type Sima (Fig. 6E), but nevertheless, under conditions in which the system was not fully active—in normoxic transgenic embryos—the activity of Sima mutated variants was remarkably higher than that of wild-type Sima protein (Fig. 6G and H).

To investigate whether export-dependent regulation of Sima impinges on the expression of endogenous target genes, we analyzed by mRNA in situ hybridization the expression of the HIF prolyl-4-hydroxylase Fatiga, which was previously described as a bona fide Sima endogenous target (8, 31). As shown in Fig. 6I, the expression of *fatiga* induced by L101A and M115A Sima mutants was clearly stronger than its expression induced by wild-type Sima; as expected, SimaΔHLH completely failed to induce *fatiga*. Taken together, the above experiments indicate that regulation of Sima nuclear export contributes to the regulation of its transcriptional activity.

Evolutionary conservation of NES1 and NES2 in the bHLH-PAS protein family. Having identified two functional NESs in the bHLH domain of Sima, we were interested in determining whether these NESs are present in other *Drosophila* bHLH-PAS proteins. Sequence alignment revealed that, indeed, nuclear export signals homologous to Sima NES1 and NES2 exist in the bHLH domain of many other *Drosophila* bHLH-PAS transcription factors (Fig. 7A), suggesting that nuclear export could be a general regulatory feature of this protein family. To investigate this possibility, we analyzed the ability of the HLH motifs of different bHLH-PAS proteins to promote CRM1-dependent nuclear export of an EGFP reporter in transfected S2 cells (Fig. 7B to H). As shown in Fig. 7C to F, subcellular localization of the HLH-EGFP chimeras corresponding to Cycle, Trachealess, Dysfusion, or Single minded, all of them displaying at least one NES in the bHLH domain (Fig. 7A), all exhibited a localization clearly more cytoplasmic than that of the EGFP control construct (Fig. 7B to F and I), paralleling subcellular localization of EGFP-SimaHLH (Fig. 4H and 7I). Upon LMB treatment, subcellular localization of Sima, Cycle, Trachealess, Dysfusion, and Single minded EGFP chimeras shifted to a predominantly nuclear localization (Fig. 4H and 7C to F and I), while the EGFP negative control (Fig. 7B), as well as EGFP-Tango-HLH and EGFP-Clock (Fig. 7G and H), the two latter lacking predicted NESs at the bHLH domain (Fig. 7A), were unaffected by the addition of LMB (Fig. 7I). These results suggest that those *Drosophila* bHLH-PAS proteins that include either NES1 alone, or both NES1 and NES2 presumptive NESs are likely regulated by CRM1-mediated nuclear export.

DISCUSSION

Subcellular localization of Sima is controlled by CRM1-dependent nuclear export. By combining cell culture strategies with experiments in living embryos, we have shed light on the mechanisms involved in the regulation of subcellular localization of the *Drosophila* HIF-α homologue, Sima. We have characterized the nuclear localization signal required for Sima nuclear import and found a bipartite NLS localized next to the Sima C terminus which displays an atypical separation between the two stretches of basic amino acids (14 residues instead of the 10-aa usual separation in canonical bipartite NLSs). Interestingly, the structure and position of this functional NLS seem to be a conserved aspect of HIF-α subunits, since nuclear import of mammalian HIF-1α, -2α, and -3α proteins also depends on C-terminal bipartite NLSs in which the two stretches of basic amino acids display a longer-than-normal separation (32).

We have shown that the Sima protein shuttles continuously between the nucleus and the cytoplasm and that nuclear export is mediated, at least in part, by the nuclear export receptor CRM1.

We demonstrated that the HLH motif of Sima encompasses two CRM1 consensus sequences, NES1 and NES2, that are critically required for Sima steady-state subcellular localization. We performed an in vivo nuclear export assay and showed that when embryos are exposed to extreme hypoxic conditions (1% O_2), Sima accumulates totally in the nuclear compartment, and after reoxygenation it is completely exported to the cytoplasm within only 10 min, through a mechanism that involves NES1 and NES2. Sequence comparisons have led to the identification of homologous NESs in the HLH domain of HIF-1α homologues from diverse phylogenetic groups, including insects, fish, amphibians, birds, and mammals, while they are absent from all HIF-β subunits. Reports on mammalian HIF-α provided circumstantial evidence that CRM1-dependent nuclear export might also occur in mammalian HIF-α (3, 38). However, detailed studies suggested that CRM1 does not play a role in mammalian HIF-α subunit subcellular localization but, rather, is exported from the nucleus to the cytoplasm through a mechanism that depends on the tumor suppressor factor VHL (17), which is known to shuttle between the nucleus and the cytoplasm, in a CRM1-independent manner (4). The fact that nuclear export of a Sima protein variant that lacks the entire HLH domain was slowed down but not totally abrogated supports the possibility that Sima is subjected to CRM1-independent nuclear export as well. Thus, CRM1-dependent and CRM1-independent nuclear export mechanisms apparently coexist to cooperate in determining the oxygen-dependent steady-state subcellular localization of Sima, as well as its rapid nuclear clearance upon reoxygenation.

How does hypoxia impinge on nuclear export? This point is so far unclear. We could verify that subcellular localization of EGFP-SimaHLH is not influenced by oxygen levels (data not shown). Thus, it seems that, although the HLH motif is criti-

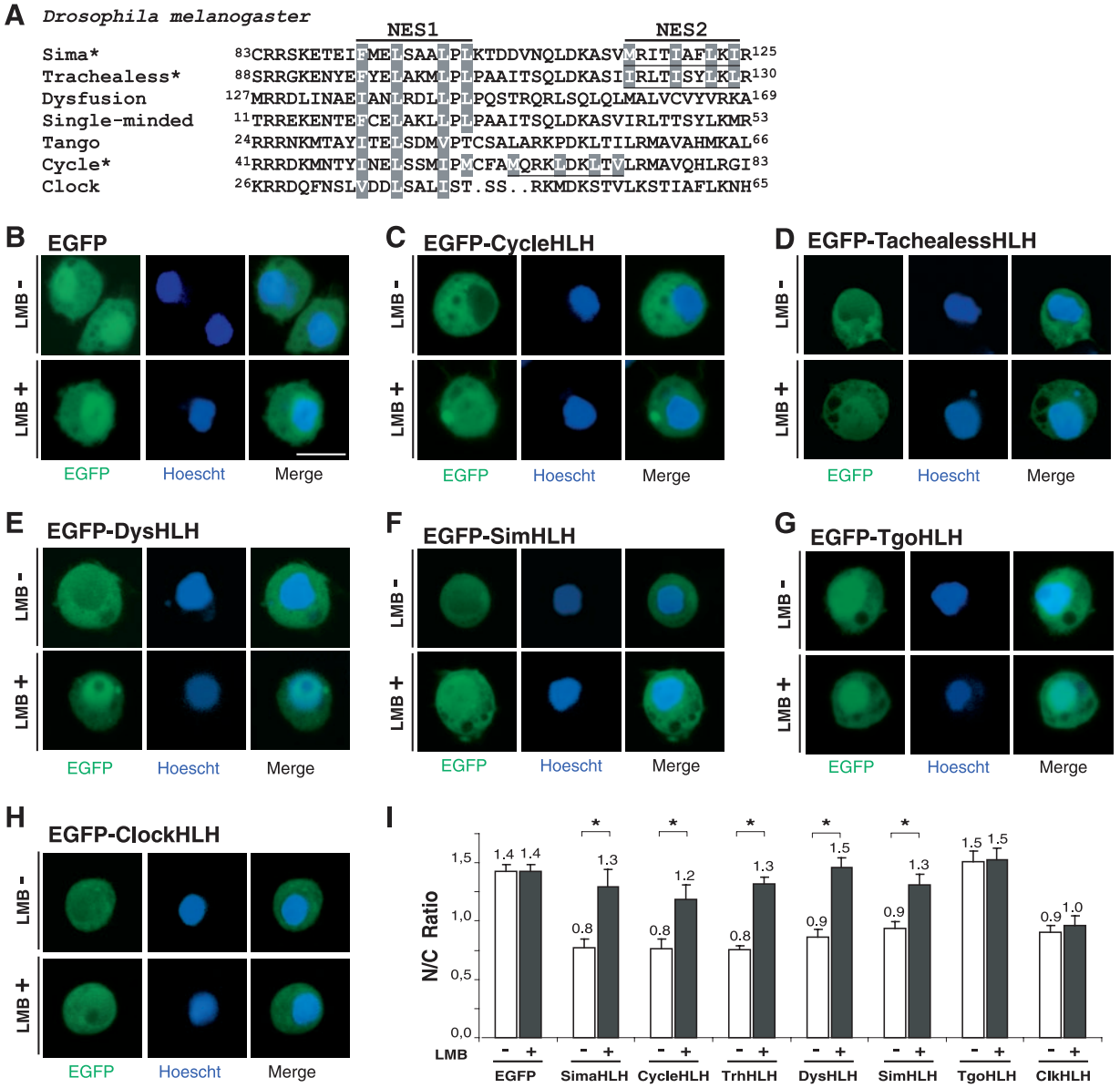

FIG. 7. NES1 and NES2 are conserved in the bHLH domain of other bHLH-PAS proteins. (A) Sequence alignment of the bHLH domain of several *Drosophila* proteins. The hydrophobic residues that define the CRM1 recognition consensus are highlighted with gray boxes. Note that in the Cycle sequence the position of NES2 (underlined) is shifted toward the N terminus within helix 2. (B to H) EGFP was fused to the HLH motif of several different bHLH-PAS proteins, and constructs were transiently transfected in S2 cells. Subcellular localization of the chimeras was studied after adding or not 30 nM LMB. Bar, 10 μm. (I) At least 10 cells from each construct and condition were quantitatively analyzed with a confocal microscope by measuring the intensity of EGFP fluorescence per μm^2 in the nucleus (N) and cytoplasm (C); the N/C ratio is represented (*, $P < 10^{-4}$, Student's t test; $n > 10$).

cally required for nuclear export, this motif is not sufficient for oxygen-dependent regulation of nuclear export. It remains to be defined which regions of the protein are responsible for oxygen-dependent sensitivity of Sima nuclear export.

Nuclear export as a mechanism to control Sima activity. We have shown that by altering one out of the four hydrophobic amino acids that define each of the CRM1-dependent NES consensus sequences in the Sima bHLH domain, it is possible to impair nuclear export and increase Sima transcriptional activity. These results suggest that nuclear export plays a role in oxygen-dependent control of Sima activity, adding a new layer to the complexity of the regulation of this protein (Fig. 8). How does this new mode of regulation interface with the well-characterized machinery that controls proteasomal degradation of HIF-α proteins? So far, this point is unclear. It has not been fully established whether proteasomal degradation of HIF-α proteins occurs in the nucleus, in the cytoplasm, or if it can take place in both compartments (3, 57). It is conceivable that Sima needs first to be exported from the nucleus in order to be degraded in the cytoplasm (17). Alternatively, proteasomal degradation and nuclear export could represent two parallel mechanisms that synergize in shutting off transcriptional

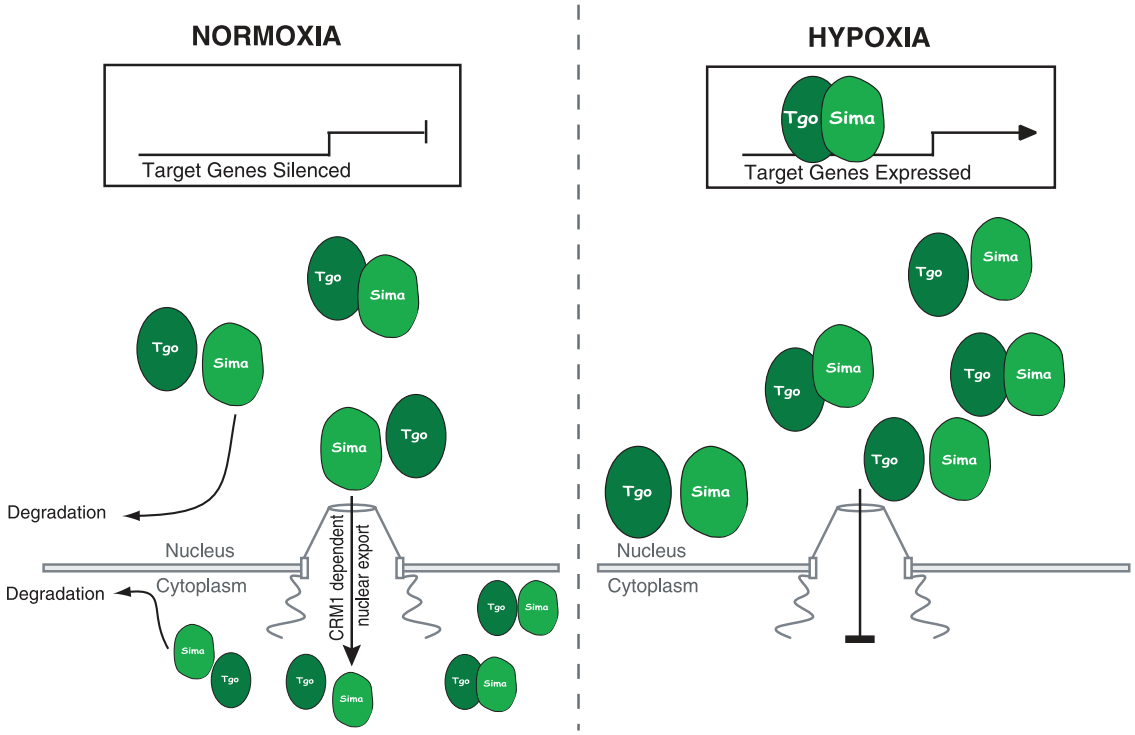

FIG. 8. Model for Sima regulation by CRM1 nuclear export. In normoxia, the nuclear export receptor CRM1 promotes Sima nuclear export, contributing to target gene silencing. In hypoxia, Sima fails to be exported to the cytoplasm, resulting in nuclear accumulation and target gene induction.

activity under normoxic conditions. Consistent with this possibility, regulation of the activity of many transcription factors often occurs at several different levels through partially redundant mechanisms that operate simultaneously to ensure precise control of their activity. If this were the case, Sima degradation and nuclear export would occur simultaneously in an oxygen-dependent manner to act synergistically in the reduction of nuclear levels of the transcription factor, thereby contributing to prevent hypoxia-inducible gene expression.

Two conserved nuclear export signals in the bHLH domain of many bHLH-PAS proteins. Sequence alignment has revealed the occurrence of one CRM1-dependent NES in each of the two α-helices of the bHLH domain in several *Drosophila* bHLH-PAS proteins (Fig. 7A). In the mammalian aryl hydrocarbon receptor (Ahr), these CRM1-dependent NESs have been shown to be functional (19, 41); our studies extend this observation to other members of the family, suggesting that regulation based on nuclear export is probably a hallmark of a subgroup of these transcription factors. Analysis of the subcellular localization of some *Drosophila* EGFP-HLH fusion chimeras suggest that these presumptive NESs might indeed be functional, as they can promote nuclear export of the EGFP reporter.

Interestingly, NES1 and NES2 occur in the bHLH domain of the *Drosophila* proteins Sima, Cycle, and Trachealess, whereas only NES1 occurs in the bHLH-PAS proteins Single-minded and Dysfusion. While NES1 and NES2 are both required for Sima normal nuclear export, NES1 by itself seems to be sufficient for driving nuclear export of Dysfusion and Single-minded.

What might be the physiological meaning of the conservation of nuclear export in members of the bHLH-PAS family? This mechanism might certainly contribute to the regulation of members of the family that are controlled by external stimuli, such as the mammalian Ahr, which is activated by xenobiotic ligands (41), or Sima, which mediates adaptation to environmental oxygen tension. Interestingly, subcellular localization of the master regulator of tracheal development, Trachealess, which is not primarily involved in adaptation to environmental stimuli, has been reported to be regulated by the activity of the phosphatidylinositol 3-kinase/Akt pathway (22). Thus, it is conceivable that other bHLH-PAS members, such as the circadian protein Cycle or other bHLH-PAS proteins primarily involved in developmental processes, such as Single minded and Dysfusion, might be subjected to regulation of subcellular localization as well. Further research is required to determine to what extent CRM1-dependent nuclear export is a common feature in the regulation of bHLH-PAS proteins.

ACKNOWLEDGMENTS

We are grateful to Alejandro Colman-Lerner for help and advice with yeast two-hybrid experiments, Steve Crews for reagents, the Bloomington Stock Center for fly stocks, to members of the Wappner and Ceriani labs for fruitful discussions, and to Manuel de la Mata for critical reading of the manuscript.

This work was supported by Wellcome Trust grant 070161/Z/03/Z, Universidad de Buenos Aires X411 and ANPCyT 01-10839 to P.W. N.M.R. and M.I. are doctoral fellows of CONICET; A.C. and P.W. are career investigators of CONICET; P.W. is a Howard Hughes Medical Institute International Scholar.

REFERENCES

1. **Bacon, N. C., P. Wappner, J. O'Rourke, S. M. Bartlett, B. Shilo, C. W. Pugh, and P. J. Ratcliffe.** 1998. Regulation of the Drosophila bHLH-PAS protein Sima by hypoxia: functional evidence for homology with mammalian HIF-1 alpha. Biochem. Biophys. Res. Commun. **249:**811–816.
2. **Begitt, A., T. Meyer, M. van Rossum, and U. Vinkemeier.** 2000. Nucleocytoplasmic translocation of Stat1 is regulated by a leucine-rich export signal in the coiled-coil domain. Proc. Natl. Acad. Sci. USA **97:**10418–10423.
3. **Berra, E., D. Roux, D. E. Richard, and J. Pouyssegur.** 2001. Hypoxia-inducible factor-1 alpha (HIF-1 alpha) escapes O_2-driven proteasomal degradation irrespective of its subcellular localization: nucleus or cytoplasm. EMBO Rep. **2:**615–620.
4. **Bonicalzi, M. E., I. Groulx, N. de Paulsen, and S. Lee.** 2001. Role of exon 2-encoded beta-domain of the von Hippel-Lindau tumor suppressor protein. J. Biol. Chem. **276:**1407–1416.
5. **Brand, A. H., and N. Perrimon.** 1993. Targeted gene expression as means of altering cell fates and generating dominant phenotypes. Development **118:** 401–415.
6. **Brar, S. S., M. Watson, and M. Diaz.** 2004. Activation-induced cytosine deaminase (AID) is actively exported out of the nucleus but retained by the induction of DNA breaks. J. Biol. Chem. **279:**26395–26401.
7. **Bruick, R. K., and S. L. McKnight.** 2001. A conserved family of prolyl-4-hydroxylases that modify HIF. Science **294:**1337–1340.
8. **Centanin, L., P. J. Ratcliffe, and P. Wappner.** 2005. Reversion of lethality and growth defects in Fatiga oxygen-sensor mutant flies by loss of hypoxia-inducible factor-alpha/Sima. EMBO Rep. **6:**1070–1075.
9. **Chilov, D., G. Camenisch, I. Kvietikova, U. Ziegler, M. Gassmann, and R. H. Wenger.** 1999. Induction and nuclear translocation of hypoxia-inducible factor-1 (HIF-1): heterodimerization with ARNT is not necessary for nuclear accumulation of HIF-1α. J. Cell Sci. **112:**1203–1212.
10. **Crews, S. T., and C. M. Fan.** 1999. Remembrance of things PAS: regulation of development by bHLH-PAS proteins. Curr. Opin. Genet. Dev. **9:**580–587.
11. **Cuff, J. A., and G. J. Barton.** 2000. Application of multiple sequence alignment profiles to improve protein secondary structure prediction. Proteins **40:**502–511.
12. **Dekanty, A., S. Lavista-Llanos, M. Irisarri, S. Oldham, and P. Wappner.** 2005. The insulin-PI3K/TOR pathway induces a HIF-dependent transcriptional response in Drosophila by promoting nuclear localization of HIF-alpha/Sima. J. Cell Sci. **118:**5431–5441.

12a. **Dignam, J. D., R. M. Lebovitz, and R. G. Roeder.** 1983. Accurate transcriptional initiation by RNA polymerase II in a soluble extract from isolated mammalian nuclei. Nucleic Acids Res. **11:**1475–1489.

13. **Douglas, R. M., and G. G. Haddad.** 2003. Genetic models in applied physiology: invited review: effect of oxygen deprivation on cell cycle activity: a profile of delay and arrest. J. Appl. Physiol. **94:**2068–2083.
14. **Epstein, A. C., J. M. Gleadle, L. A. McNeill, K. S. Hewitson, J. O'Rourke, D. R. Mole, M. Mukherji, E. Metzen, M. I. Wilson, A. Dhanda, Y. M. Tian, N. Masson, D. L. Hamilton, P. Jaakkola, R. Barstead, J. Hodgkin, P. H. Maxwell, C. W. Pugh, C. J. Schofield, and P. J. Ratcliffe.** 2001. C. elegans EGL-9 and mammalian homologs define a family of dioxygenases that regulate HIF by prolyl hydroxylation. Cell **107:**43–54.
15. **Fornerod, M., M. Ohno, M. Yoshida, and I. W. Mattaj.** 1997. CRM1 is an export receptor for leucine-rich nuclear export signals. Cell **90:**1051–1060.
16. **Gorr, T. A., T. Tomita, P. Wappner, and H. F. Bunn.** 2004. Regulation of Drosophila hypoxia-inducible factor (HIF) activity in SL2 cells: identification of a hypoxia-induced variant isoform of the HIFα homolog gene similar. J. Biol. Chem. **279:**36048–36058.
17. **Groulx, I., and S. Lee.** 2002. Oxygen-dependent ubiquitination and degradation of hypoxia-inducible factor requires nuclear-cytoplasmic trafficking of the von Hippel-Lindau tumor suppressor protein. Mol. Cell. Biol. **22:**5319–5336.
18. **Henderson, B. R., and A. Eleftheriou.** 2000. A comparison of the activity, sequence specificity, and CRM1-dependence of different nuclear export signals. Exp. Cell. Res. **256:**213–224.
19. **Ikuta, T., J. Watanabe, and K. Kawajiri.** 2002. Characterization of the LxxLL motif in the aryl hydrocarbon receptor: effects on subcellular localization and transcriptional activity. J. Biochem. **131:**79–85.
20. **Isaac, D. D., and D. J. Andrew.** 1996. Tubulogenesis in Drosophila: a requirement for the Trachealess gene product. Genes Dev. **10:**103–117.
21. **Jiang, L., and S. T. Crews.** 2003. The *Drosophila* dysfusion basic helix-loop-helix (bHLH)-PAS gene controls tracheal fusion and levels of the Trachealess bHLH-PAS protein. Mol. Cell. Biol. **23:**5625–5637.
22. **Jin, J., N. Anthopoulos, B. Wetsch, R. C. Binari, D. D. Isaac, D. J. Andrew, J. R. Woodgett, and A. S. Manoukian.** 2001. Regulation of Drosophila tracheal system development by protein kinase B. Dev. Cell **1:**817–827.
23. **Jones, D. T.** 1999. Protein secondary structure prediction based on position-specific scoring matrices. J. Mol. Biol. **292:**195–202.
24. **Kalderon, D., W. D. Richardson, A. F. Markham, and A. E. Smith.** 1984. Sequence requirements for nuclear location of simian virus 40 large-T antigen. Nature **311:**33–38.
25. **Kallio, P. J., K. Okamoto, S. O'Brien, P. Carrero, Y. Makino, H. Tanaka, and L. Poellinger.** 1998. Signal transduction in hypoxic cells: inducible nuclear translocation and recruitment of the CBP/p300 coactivator by the hypoxia-inducible factor-1α. EMBO J. **17:**6573–6586.
26. **Kewley, R. J., M. L. Whitelaw, and A. Chapman-Smith.** 2004. The mammalian basic helix-loop-helix/PAS family of transcriptional regulators. Int. J. Biochem. Cell. Biol. **36:**189–204.
27. **Komeili, A., and E. K. O'Shea.** 2001. New perspectives on nuclear transport. Annu. Rev. Genet. **35:**341–364.
28. **Kudo, N., N. Matsumori, H. Taoka, D. Fujiwara, E. P. Schreiner, B. Wolff, M. Yoshida, and S. Horinouchi.** 1999. Leptomycin B inactivates CRM1/exportin 1 by covalent modification at a cysteine residue in the central conserved region. Proc. Natl. Acad. Sci. USA **96:**9112–9117.
29. **la Cour, T., L. Kiemer, A. Molgaard, R. Gupta, K. Skriver, and S. Brunak.** 2004. Analysis and prediction of leucine-rich nuclear export signals. Protein Eng. Des. Sel. **17:**527–536.
30. **Lacroix, E., A. R. Viguera, and L. Serrano.** 1998. Elucidating the folding problem of alpha-helices: local motifs, long-range electrostatics, ionic-strength dependence and prediction of NMR parameters. J. Mol. Biol. **284:**173–191.
31. **Lavista-Llanos, S., L. Centanin, M. Irisarri, D. M. Russo, J. M. Gleadle, S. N. Bocca, M. Muzzopappa, P. J. Ratcliffe, and P. Wappner.** 2002. Control of the hypoxic response in *Drosophila melanogaster* by the basic helix-loop-helix PAS protein Similar. Mol. Cell. Biol. **22:**6842–6853.
32. **Luo, J. C., and M. Shibuya.** 2001. A variant of nuclear localization signal of bipartite-type is required for the nuclear translocation of hypoxia inducible factors (1α, 2α, and 3α). Oncogene **20:**1435–1444.
33. **Mattaj, I. W., and L. Englmeier.** 1998. Nucleocytoplasmic transport: the soluble phase. Annu. Rev. Biochem. **67:**265–306.
34. **Maxwell, P. H., M. S. Wiesener, G. W. Chang, S. C. Clifford, E. C. Vaux, M. E. Cockman, C. C. Wykoff, C. W. Pugh, E. R. Maher, and P. J. Ratcliffe.** 1999. The tumour suppressor protein VHL targets hypoxia-inducible factors for oxygen-dependent proteolysis. Nature **399:**271–275.
35. **McBride, K. M., C. McDonald, and N. C. Reich.** 2000. Nuclear export signal located within the DNA-binding domain of the STAT1transcription factor. EMBO J. **19:**6196–6206.

35a. **Mendelsohn, A. R., and R. Brent.** 1994. Applications of interaction traps/two-hybrid systems to biotechnology research. Curr. Opin. Biotechnol. **5:**482–486.

36. **Michel, G., E. Minet, I. Ernest, I. Roland, F. Durant, J. Remacle, and C. Michiels.** 2000. A model for the complex between the hypoxia-inducible factor-1 (HIF-1) and its consensus DNA sequence. J. Biomol. Struct. Dyn. **18:**169–179.
37. **Morgenstern, B., and W. R. Atchley.** 1999. Evolution of bHLH transcription factors: modular evolution by domain shuffling? Mol. Biol. Evol. **16:**1654–1663.
38. **Mylonis, I., G. Chachami, M. Samiotaki, G. Panayotou, E. Paraskeva, A. Kalousi, E. Georgatsou, S. Bonanou, and G. Simos.** 2006. Identification of MAPK phosphorylation sites and their role in the localization and activity of hypoxia-inducible factor-1α. J. Biol. Chem. **281:**33095–33106.
39. **Nambu, J. R., W. Chen, S. Hu, and S. T. Crews.** 1996. The Drosophila melanogaster Similar bHLH-PAS gene encodes a protein related to human hypoxia-inducible factor 1 alpha and Drosophila Single-minded. Gene **172:** 249–254.
40. **Poellinger, L., and R. S. Johnson.** 2004. HIF-1 and hypoxic response: the plot thickens. Curr. Opin. Genet. Dev. **14:**81–85.
41. **Pollenz, R. S., and E. R. Barbour.** 2000. Analysis of the complex relationship between nuclear export and aryl hydrocarbon receptor-mediated gene regulation. Mol. Cell. Biol. **20:**6095–6104.
42. **Pongratz, I., C. Antonsson, M. L. Whitelaw, and L. Poellinger.** 1998. Role of the PAS domain in regulation of dimerization and DNA binding specificity of the dioxin receptor. Mol. Cell. Biol. **18:**4079–4088.
43. **Robbins, J., S. M. Dilworth, R. A. Laskey, and C. Dingwall.** 1991. Two interdependent basic domains in nucleoplasmin nuclear targeting sequence: identification of a class of bipartite nuclear targeting sequence. Cell **64:**615–623.
44. **Rost, B., G. Yachdav, and J. Liu.** 2004. The PredictProtein server. Nucleic Acids Res. **32:**W321–W326.
45. **Roth, P., N. Xylourgidis, N. Sabri, A. Uv, M. Fornerod, and C. Samakovlis.** 2003. The Drosophila nucleoporin DNup88 localizes DNup214 and CRM1 on the nuclear envelope and attenuates NES-mediated nuclear export. J. Cell Biol. **163:**701–706.
46. **Sang, N., J. Fang, V. Srinivas, I. Leshchinsky, and J. Caro.** 2002. Carboxyl-terminal transactivation activity of hypoxia-inducible factor 1 alpha is governed by a von Hippel-Lindau protein-independent, hydroxylation-regulated association with p300/CBP. Mol. Cell. Biol. **22:**2984–2992.
47. **Sonnenfeld, M., M. Ward, G. Nystrom, J. Mosher, S. Stahl, and S. Crews.** 1997. The Drosophila tango gene encodes a bHLH-PAS protein that is orthologous to mammalian Arnt and controls CNS midline and tracheal development. Development **124:**4571–4582.
48. **Stade, K., C. S. Ford, C. Guthrie, and K. Weis.** 1997. Exportin 1 (Crm1p) is an essential nuclear export factor. Cell **90:**1041–1050.
49. **Tanimoto, K., Y. Makino, T. Pereira, and L. Poellinger.** 2000. Mechanism of regulation of the hypoxia-inducible factor-1 alpha by the von Hippel-Lindau tumor suppressor protein. EMBO J. **19:**4298–4309.

50. **Wang, G. L., B. H. Jiang, E. A. Rue, and G. L. Semenza.** 1995. Hypoxia-inducible factor 1 is a basic-helix-loop-helix-PAS heterodimer regulated by cellular O2 tension. Proc. Natl. Acad. Sci. USA **92:**5510–5514.
51. **Weitzman, J. B.** 16 February 2005, posting date. Dishevelled nuclear shuttling. J. Biol. **4:**1.doi:10.1186/jbiol21.
52. **Wen, W., A. T. Harootunian, S. R. Adams, J. Feramisco, R. Y. Tsien, J. L. Meinkoth, and S. S. Taylor.** 1994. Heat-stable inhibitors of cAMP-dependent protein kinase carry a nuclear export signal. J. Biol. Chem. **269:**32214–32220.
53. **Wharton, K. A., Jr., R. G. Franks, Y. Kasai, and S. T. Crews.** 1994. Control of CNS midline transcription by asymmetric E-box-like elements: similarity to xenobiotic responsive regulation. Development **120:**3563–3569.
54. **Wilk, R., I. Weizman, and B. Z. Shilo.** 1996. trachealess encodes a bHLH-PAS protein that is an inducer of tracheal cell fates in Drosophila. Genes Dev. **10:**93–102.
55. **Yu, F., S. B. White, Q. Zhao, and F. S. Lee.** 2001. HIF-1α binding to VHL is regulated by stimulus-sensitive proline hydroxylation. Proc. Natl. Acad. Sci. USA **98:**9630–9635.
56. **Zelzer, E., P. Wappner, and B. Z. Shilo.** 1997. The PAS domain confers target gene specificity of Drosophila bHLH/PAS proteins. Genes Dev. **11:**2079–2089.
57. **Zheng, X., J. L. Ruas, R. Cao, F. A. Salomons, Y. Cao, L. Poellinger, and T. Pereira.** 2006. Cell-type-specific regulation of degradation of hypoxia-inducible factor 1 alpha: role of subcellular compartmentalization. Mol. Cell. Biol. **26:**4628–4641.